IMPROVING THE EFFICIENCY, STABILITY, AND OPTICAL PROPERTIES OF PEROVSKITE SOLAR CELLS THROUGH OPTIMIZATION OF THE HOLE-TRANSPORT LAYER

Tazhibayev S.K., Academician E.A. Buketov Karaganda University, Karaganda, Kazakhstan
Berik A.A., Academician E.A. Buketov Karaganda University, Karaganda, Kazakhstan
Bokanova A.A., Academician E.A. Buketov Karaganda University, Karaganda, Kazakhstan
Beisembekov M.K., Academician E.A. Buketov Karaganda University, Karaganda, Kazakhstan
Zeinidenov A.K., Academician E.A. Buketov Karaganda University, Karaganda, Kazakhstan

Abstract

Perovskite solar cells (PSCs) have emerged as a leading technology in the photovoltaic sector due to their high efficiency and low fabrication cost. However, the performance and stability of PSCs are often limited by the properties of hole transport layers (HTLs). In this study, we explore the use of cobalt phthalocyanine (CoPc) and a composite CoPc/Spiro-OMeTAD layer as HTLs to enhance the efficiency and stability of PSCs. Optical studies demonstrated that these composite layers maintain high transparency while providing effective light absorption. Photoelectrical characterizations showed that PSCs with the CoPc/Spiro-OMeTAD HTLs achieved a power conversion efficiency (PCE) of 18.7%, outperforming devices with standard Spiro-OMeTAD and single CoPc layers. Moreover, the composite HTLs improved the stability of the PSCs, retaining 84% of the initial PCE after 300 hours of operation without encapsulation. Impedance spectroscopy indicated that the composite HTLs reduce charge transfer resistance while maintaining lower recombination rates. These findings suggest that CoPc/Spiro-OMeTAD composite layers are promising candidates for enhancing both the efficiency and stability of PSCs.

Keywords: perovskite solar cells, Spiro-OMeTAD, cobalt phthalocyanine, hole transport layers, optical properties, V-I characteristics, impedance spectroscopy.

1. Introduction

The unprecedented development of PSCs is due to their relatively low cost, ease of fabrication, and great potential for achieving higher efficiency than c-Si solar cells [1-3]. To improve the efficiency and stability of PSCs, various studies are being carried out to optimize the composition and structure of all layers of PSCs, especially charge transport layers. Currently, the PCE of PSCs has reached more than 25%. These highly efficient PSCs are based on Spiro-OMeTAD hole transport layers [4-6]. Despite the record PCE have been achieved by using Spiro-OMeTAD HTLs, this material has limited hole mobility (≈10-4 cm2V-1s-1) and low electrical conductivity (≈10-8 Scm-1), which limits further boost up of device performance. In addition, Spiro-OMeTAD is expensive materials, has low stability, and its deposition on a perovskite layer is considered technologically complicated, which is a major obstacle for large-scale application [7]. The efficacy of using MPc in PSCs has been confirmed by several research groups. Duong T. et al. designed MPc based PSCs with PCE as high as 20%. It was achieved by depositing a CuPc layer on a perovskite film with a certain orientation [8].

In this paper, we use CoPc layer and composite CoPc/Spiro-OMeTAD layers as a hole transport layer of PSCs. The effects of the CoPc intermediate layer on charge transport in PSCs and stability of device were investigated. The proposed composite CoPc/Spiro-OMeTAD HTLs demonstrated the improvement in photovoltaic performance and operational stability of PSCs.

2. Materials and Methods

2.1. The fabrication of PSCs

PSCs were fabricated on glass substrates with a Fluoride Tin Oxide (FTO) layer (15 Ω/cm²), serving as the cathode. Substrates were cleaned in acetone, hot deionized water, and 2-propanol, followed by UV-ozone treatment. The electron transport layer (ETL) TiO_2 was deposited by spin coating Ti-Nanoxide BL/SC-Solaronix solution (SPIN150i, 5000 rpm, 30 s), then annealed at 500 °C for 1 h.

Perovskite films were prepared from $PbCl_2$ (230 mg) and MAI (394 mg) dissolved in 1 ml DMF, stirred at 60 °C for 2 h. After deposition, films were annealed at 100 °C for 2 h, with color change from yellow to dark brown confirming crystallization.

As hole-transport layers (HTLs), Spiro-OMeTAD and cobalt phthalocyanine (CoPc, Sigma-Aldrich) were used. CoPc was thermally evaporated in vacuum (CY-1700x-sps-2, pressure $\leq 10^{-5}$ Pa, rate <1 nm/s). Spiro-OMeTAD was prepared from 75 mg in 1 ml chlorobenzene, stirred at 30 °C for 1 h, and deposited at 5000 rpm. For comparison, cells with CoPc HTLs and with an intermediate layer between Spiro-OMeTAD and Ag were fabricated.

Finally, Ag electrodes were vacuum-deposited (10^{-3} Pa). All steps, including perovskite formation, were carried out in a nitrogen-filled glove box. Structural formulas (Spiro-OMeTAD, CoPc) and PSC configuration/energy diagram are shown in Fig. 1a–c.

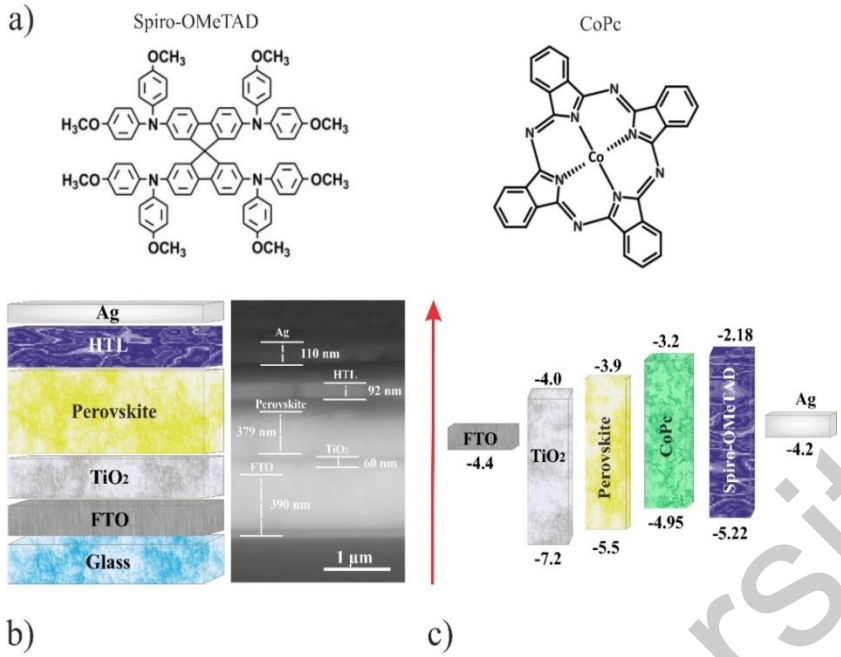

Figure1. Structural formula (a), cell configuration (b) and energy diagram of a perovskite solar cell (c).

2.2. Analysis methods

The absorption and transmission spectra were recorded using an AvaSpec-ULS2048CL-EVO spectrometer (Avantes). A combined deuterium-halogen light source AvaLight-DHc (Avantes) with an operating spectral range of 200-2500 nm was used as probing radiation.

The current-voltage characteristics of solar cells were measured using a PVIV-1A setup (Newport, Canada). A Sol3A solar energy simulator (class AAA, Newport, Canada) with a radiation intensity of 100 mW/cm^2 was used as a light source.

The impedance spectra were measured using a P-45X potentiostat-galvanostat (Elins, Russia) with an additional FRA-24M frequency analyzer module installed to measure the electrophysical characteristics on alternating current.

3. Results and Discussion

3.1 Optical properties

Figure 2a presents the absorption spectra of Spiro-OMeTAD, CoPc, CoPc/Spiro-OMeTAD and Spiro-OMeTAD/CoPc layers. The Spiro-OMeTAD layer shows an intense absorption the range from 350 to 430 nm (λmax = 377 nm), which is characteristic absorption of Spiro-OMeTAD. In the absorption spectra of CoPc there are three intense bands with λ_{max} = 360 nm (CoPc band or B-range), which correspond to mixed π-π* and n-π transitions a2u→2eg and b2u→2eg. In the Q-range, two maxima are observed at wavelengths λmax = 630 nm and λmax = 688 nm, which corresponds to the π-π* transition a1u→2eg. When measuring the CoPc/Spiro-OMeTAD and Spiro-OMeTAD/CoPc films, a decrease in the intensity of the Q-band absorption spectra is observed. The optical transmission spectra of the films in the range of 300 - 800 nm are shown in Figure 2b. The average transmittance was about 83-95%, the obtained data show that all the films have high transparency.

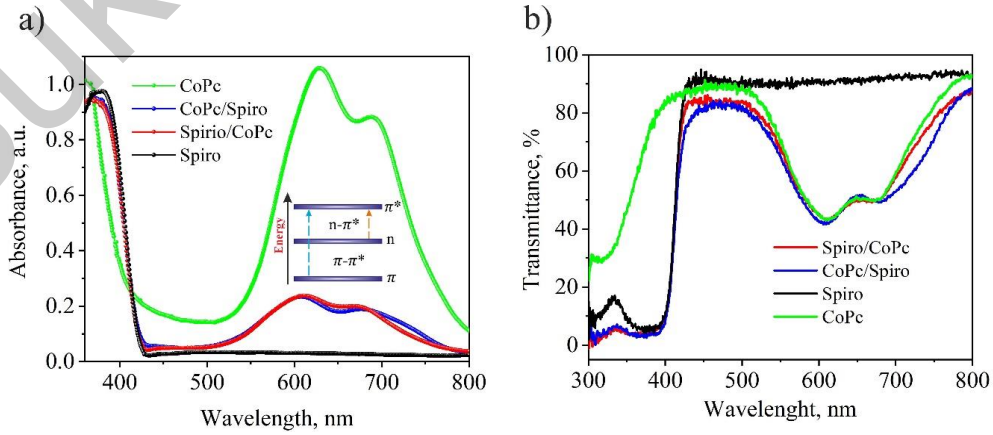

Figure 2. Absorption and transmission spectra of films with different layers.

3.2. Photoelectrical characterizations

Figure 3a shows the current-voltage characteristics of the PSCs with different HTLs. The photovoltaic performance of the PSCs are shown in Table 1. From the Table 1, we observe that the PCS with CoPc/Spiro-OMeTAD composite HTLs possesses highest PCE (18.7%.) with short-circuit current density (J_{sc}) of 22.3 mA/cm^2, open-circuit voltage (V_{oc}) of 1 V, fill factor (FF) of 0.84. For comparison, PSCs with a standard Spiro-OMeTAD layer has lower performance. The deice with the Spiro-OMeTAD HTLs showed a PCE as high as 16.5% with a Jsc of 21.5 mA/cm^2, a V_{oc} of 1 V, and a FF of 0.77. PSCs with a CoPc layer placed between the Spiro-OMeTAD and the Ag electrode demonstrated even lower PCE (14.5%) with at J_{sc} of 20.9 mA/cm^2, V_{oc} of 1 V and FF 0.70. The device with single CoPc HTLs shoed the worst photovoltaic parameters (J_{sc} of 20.2 mA/cm^2, V_{oc} of 9.93V, FF of 0.66 and PCE of 13.2%).

The enhanced photovoltaic parameters of PSCs with CoPc/Spiro-OMeTAD HTL is attributed the better hole extraction efficiency and better morphology of HTLs. In studies by Bi D. et al. and Seoa Y.H. et al. were reported that PSCs with poor HTLs coating and more rough surface have severe interfacial charge recombination and hindered hole extraction. Therefore, the photovoltaic performance can be improved by the more efficient charge transport due to optimized by perovskite/HTL interface. The CoPc buffer layer improve electron blocking, Without CoPc, the holes find a conductive path from the Spiro-OMeTAD and recombine with electrons in the ETLs. The effect is aggravated by the trap states at the perovskite/Spiro-OMeTAD interface. CoPc buffer layer can passivate defect levels and minimize charge recombination.

Figure 3b shows the stability of PSCs with different HTLs configurations. The PSCs were irradiated with an AM1.5G light source, and the IV characteristics were measured every 48 h during 300 h at room temperature without encapsulation. PSCs with single Spiro-OMeTAD and single CoPc HTLs showed poor stability and their PCE dropped significantly maintaining 41% and 62% of their initial values, respectively. The device with composite Spiro-OMeTAD/CoPc HTLs showed improved stability holding 70% of the initial PCE during the test period. CoPc/Spiro-OMeTAD based PSCs showed more improved stability and managed to retain 84% of its initial PCE. This result shows that CoPc/Spiro-OMeTAD based HTLs not only improves the PCE performance, but also serves as an additional protective layer against perovskite layer degradation.

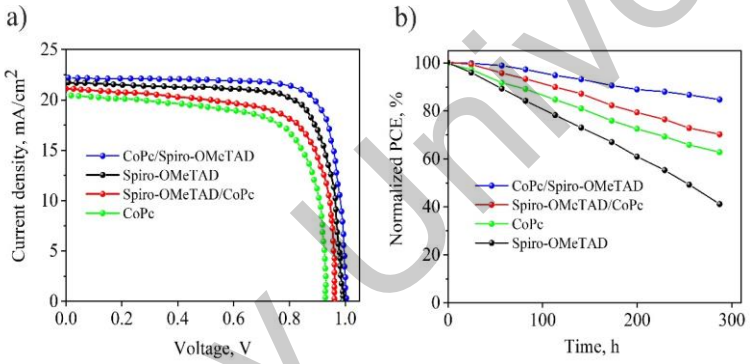

Figure 3. Current-voltage characteristics (a), stability of PSCs in air without encapsulation (b).

Table 1. Photovoltaic characteristics of perovskite solar cells

Sample	V_{oc} (V)	J_{sc}(mA/cm^2)	V_{max} (V)	J_{max}(mA/cm^2)	FF	PCE %
Spiro-OMeTAD	0.99	21.5	0.83	20.0	0.77	16.5
CoPc	0.93	20.2	0.74	17.9	0.66	13.2
CoPc/ Spiro-OMeTAD	1.00	22.3	0.88	21.5	0.84	18.7
Spiro-OMeTAD /CoPc	0.96	20.9	0.78	18.7	0.70	14.5

To understand the effect of hole transport layers on charge transfer processes in perovskite solar cells, the impedance response of the devices under small sinusoidal perturbation was measured and analyzed. Figure 4a presents the impedance spectra of PSCs with various HTLs. The dots represent the actual experimental data, while the solid lines represent the fitted data.

Generally, the impedance spectrum (IS) of PSCs consists of two semicircles: one in the high-frequency (HF) domain (kHz region) and another in the low-frequency (LF) domain (mHz-Hz region). The HF feature typically indicates processes with smaller time constants, such as charge transport resistance and capacitance at the interface between the perovskite layer and the charge transport layers. The LF region usually corresponds to processes with larger time constants, such as ionic movement within the perovskite layer and recombination processes. Such IS, showing two distinct arcs, are typically interpreted using an equivalent circuit consisting of two nested RC circuits (shown in Figure 1b), corresponding to the high and low-frequency semicircles, respectively.

The high-frequency resistance (R_{HF}) represents the charge transfer resistance at the interface, and the high-frequency capacitance (C_{HF}) represents the capacitance associated with the interface, which could be related to the dielectric properties of the materials and the space charge region and often related to the geometric capacitance of the device. The low-frequency resistance (R_{LF}) represents the recombination resistance, reflecting the rate of electron-hole recombination in the perovskite layer, while the low-frequency capacitance (C_{LF}) represents the chemical capacitance related to ionic accumulation and polarization effects within the perovskite material.

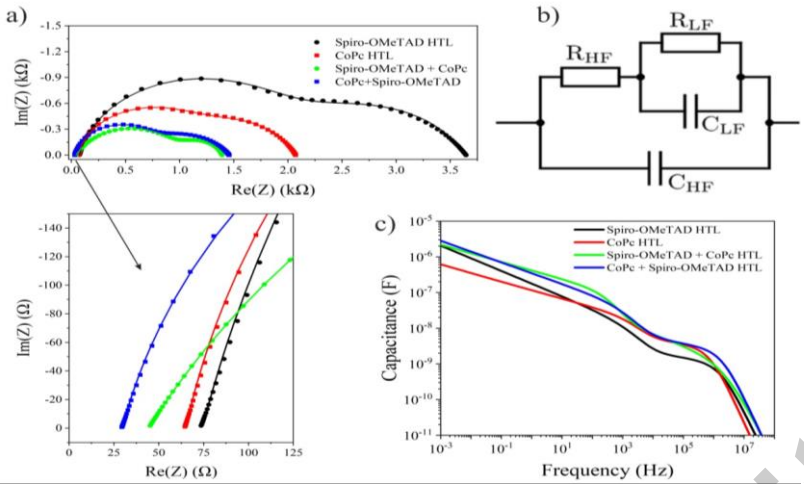

Figure 5. Impedance data of PSCs with various HTLs.
(a) Impedance spectra in the Nyquist diagram (fitted data in solid lines),
(b) equivalent circuit used to fit IS, (c) capacitance plots.

The measured IS of the PSCs with various HTLs consists of two distinctive semicircles (Figure 4a). Additionally, capacitance plots are presented in Figure 4c, showing two plateaus corresponding to the arcs in the IS Nyquist diagram. The IS were fitted using the equivalent circuit presented in Figure 5b, and the values of the circuit elements are provided in Table 2. However, instead of capacitors, constant phase elements (CPE) were used to appropriately fit the data.

Table 2. The value of electric transport parameters of perovskite solar cells

Sample	R_s (Ω)	R_{HF} (Ω)	R_{LF} (Ω)	CPE_{LF}	n (CPE_{LF})	CPE_{HF}	n (CPE_{HF})
Spiro-OMeTAD	74.23	2085	1479.0	1.59E-06	0.69	9.13E-09	0.87
CoPc	65.10	1241	763.1	1.30E-06	0.75	1.74E-08	0.89
Spiro-OMeTAD/ CoPc	44.31	989	358.4	7.46E-06	0.78	2.10E-07	0.70
CoPc/Spiro-OMeTAD	29.69	834	592.0	3.98E-06	0.69	2.28E-08	0.87

As seen from the IS and Table 2, the devices based on the composite HTLs (Spiro-OMeTAD layer followed by CoPc layer or vice versa) exhibit lower charge transfer resistance (R_{HF}) and series resistance (R_s).

4. Conclusion

This study demonstrates the potential of using CoPc and composite CoPc/Spiro-OMeTAD layers as effective HTLs in perovskite solar cells. The improved photovoltaic performance, with a maximum PCE of 18.7 %, was attributed to better hole extraction efficiency and the optimized interface between the perovskite and HTL. Additionally, the CoPc/Spiro-OMeTAD layer significantly enhanced the stability of the PSCs, maintaining 84 % of their initial efficiency after prolonged exposure to environmental conditions. Impedance spectroscopy further confirmed the advantages of the composite HTL in reducing charge transfer resistance while mitigating electron-hole recombination. Overall, the results suggest that the integration of CoPc with Spiro-OMeTAD not only boosts the efficiency of PSCs but also provides a robust approach to improving their operational stability, paving the way for more durable and efficient perovskite-based solar devices.

References

1. Kahandal S.S., Rameshwar S. T., Bobade D. S., Kim H., Piao G., Babasaheb S.R., Said Z., Pagar B.P., Pawar A.C., Kim J.M., Bulakhe R.N. Perovskite solar cells: Fundamental aspects, stability challenges, and future prospects Progress in Solid State Chemistry. Volume 74, June 2024, 100463 https://doi.org/10.1016/j.progsolidstchem.2024.100463

2. Kumar S. N., Naidu K.C.B. A review on perovskite solar cells (PSCs), materials and applications Journal of Materiomics Volume 7, Issue 5 September 2021, Pages 940-956. https://doi.org/10.1016/j.jmat.2021.04.002

3. Ma Y., Zhao Q. A strategic review on processing routes towards scalable fabrication of perovskite solar cells. Journal of Energy Chemistry Volume 64, January 2022, Pages 538-560. https://doi.org/10.1016/j.jechem.2021.05.019

4. Nakka L., Cheng Y., Aberle A.G., and Lin F. Analytical Review of Spiro-OMeTAD Hole Transport Materials: Paths Toward Stable and Efficient Perovskite Solar Cells // Adv. Energy Sustainability Res. – 2022. – Vol. 3. – P. 2200045. https://doi.org/10.1002/aesr.202200045.

5. Rombach F.M., Haque S.A. and Macdonald T.J. Lessons learned from spiro-OMeTAD and PTAA in perovskite solar cells // Energy Environ. Sci. – 2021. – Vol. 14. – P. 5161–5190. https://doi.org/10.1039/D1EE02095A.

6. X. Liu, B. Li, M Han, X. Zhang, J. Chen, S. Dai Research Progress of Self-assembled Hole-transporting Monolayers in Inverted Perovskite Solar Cells. Acta Chimica Sinica 2024, Vol. 82, Issue (3): 348-366. doi: 10.6023/A24010026

7. Heo J.H., Im S.H., Noh J.H., Mandal T.N., Lim C.S., Chang J.A., Lee Y.H., Kim H., Sarkar A., Nazeeruddin M.K., Graetzel M., Seok S.I. Efficient inorganic-organic hybrid heterojunction solar cells containing perovskite compound and polymeric hole conductors // Nat. Photon. – 2013. – Vol. 7. – P. 486–491. https://doi:10.1038/nphoton.2013.80.

8. Duong T., Peng J., Walter D., Xiang J., Shen H., Chugh D., Lockrey M., Zhong D., Li J., Weber K. Perovskite Solar Cells Employing Copper Phthalocyanine Hole-Transport Material with an Efficiency over 20% and Excellent Thermal Stability // ACS Energy Lett. – 2018. – Vol. 3. – P. 2441. https://doi.org/10.1021/acsenergylett.8b01483.

UDC 621.548.2

АЭРОДИНАМИЧЕСКИЙ АНАЛИЗ ВЛИЯНИЯ УГЛА ОТКЛОНЕНИЯ ЛОПАСТЕЙ НА ЭФФЕКТИВНОСТЬ ПАРУСНОЙ ВЕТРОЭНЕРГЕТИЧЕСКОЙ УСТАНОВКИ

Танашева Н.К. Карагандинский университет имени академика Е.А. Букетова, Карагада, Казахстан
Бурков М.А. Карагандинский университет имени академика Е.А. Букетова, Карагада, Казахстан

Анотация

В данной статье представлены результаты экспериментальных исследований парусной ветроэнергетической установки с использованием модели, управляемой системой лопастей. Основная цель исследования заключалась в изучении влияния различных параметров на аэродинамические характеристики установки. Для проведения исследований был создан экспериментальный макет установки, оснащенный парусными лопастями. Исследования проводились при различных углах отклонения парусных лопастей: 0°, 30°, 60° и 90°. Кроме того, варьировалась скорость воздушного потока в диапазоне от 3 до 15 м/с. Все эксперименты были выполнены в аэродинамической трубе Т-1-М, предназначенной для точных измерений сил и моментов, действующих на установку. Результаты исследования показали, что с увеличением скорости воздушного потока увеличивается частота вращения вала ветроэнергетической установки. Максимальная частота вращения вала достигается при нулевом отклонении парусных лопастей (α = 0°). Основные аэродинамические характеристики установки, такие как частота вращения ветротурбины, были измерены и проанализированы в зависимости от угла отклонения и скорости потока.

На основе полученных данных была построена зависимость частоты вращения парусной ветроустановки в зависимости от скорости воздушного потока. Отмечено, что с увеличением скорости потока нагрузка возрастает, что важно для оптимизации работы и эффективности ветроэнергетических установок. Таким образом, проведенные исследования предоставляют важные данные для дальнейшего совершенствования дизайна и управления парусными ветроэнергетическими установками, а также для оптимизации их работы в различных климатических условиях.

Ключевые слова: парусная лопасть, ветроэнергетическая установка, ветротурбина, угол отклонения лопастей, частота вращения, аэродинамическая труба Т-1-М.

Введение

Казахстан, благодаря своему уникальному географическому положению, обладает значительным потенциалом для использования ветроэнергетики с целью производства электроэнергии и снижения зависимости от традиционных энергоресурсов, таких как нефть и газ. В последние годы страна активно развивает эту отрасль, привлекая зарубежные инвестиции и строя новые ветропарки, что способствует достижению энергетической независимости и снижению выбросов парниковых газов. На значительной части территории Казахстана скорость ветра достигает 3-4 м/с, а на открытых участках она может достигать 6 м/с и выше [1].

Технологии в области ветроэнергетики часто включают в себя ветрогенераторы с лопастными роторами, применяемые в турбинных ветровых электростанциях. Однако такие установки сталкиваются с проблемами, связанными с непредсказуемостью скорости и направления ветра, а также ограниченным рабочим диапазоном скоростей. В Казахстане эффективность применения таких технологий сильно ограничена [2].

Одним из вариантов решения этой проблемы является использование парусных ветроэнергетических установок. В отличие от традиционных лопастных турбин, парусные установки могут генерировать электрическую энергию уже при скорости ветра 3 м/с [5]. Они работают на основе кинетической энергии ветра, которая преобразуется в механическую энергию вращения вала под воздействием аэродинамической силы подъема, действующей на поверхность паруса.

Однако существующие модели парусных ветроэнергетических установок часто не имеют механизмов регулирования угла отклонения лопастей, что снижает их эффективность при различных условиях ветра. Новизной является разработка управляемой системы лопастей в форме треугольного паруса, которая позволяет оптимизировать работу установки [6]. Это позволяет уменьшить нагрузку на установку при высоких скоростях воздушного потока и повысить ее общую эффективность.

Цель текущего исследования заключается в изучении аэродинамических характеристик парусной ветроэнергетической установки с использованием управляемой системы лопастей в форме треугольного паруса.

В данном исследовании проведены эксперименты с макетом восьмилопастной парусной ветроэнергетической установки с целью изучения влияния направления потока на аэродинамические характеристики. Данные измерялись не менее пяти раз, чтобы обеспечить надежность результатов и учесть возможные вариации в условиях эксперимента. Для проведения исследований создана ветротурбина с управляемой системой лопастей, исследования проводились в аэродинамической трубе Т-1-М со следующим условиями (Таблица1).